Published In Dalton Transactions, 2023, 52, 13235; doi.org/10.1039/D3DT02070C

Free and Coordinated Biarsolyls

Ryan M. Kirk[a] and Anthony F. Hill*[a]

A trace side product from the reaction of [Mo(AsC$_4$Me$_4$)(CO)$_3$(η-C$_5$H$_5$)] with [Mn(THF)(CO)$_2$(η^5-C$_5$H$_4$Me)] was identified as the biarsolyl complex [Mn$_2${μ-(AsC$_4$Me$_4$)$_2$}(CO)$_4$(C$_5$H$_4$Me)$_2$] on the basis of a strategic synthesis from [Mn(THF)(CO)$_2$(η^5-C$_5$H$_4$Me)] and the pre-formed and structurally characterised biarsolyl (AsC$_4$Me$_4$)$_2$. Crystallographic and computational data for this first example of a biarsolyl complex and free biarsolyls are discussed in the context of those for free biarsolyls.

Introduction

Some 266 years since Cadet launched organometallic chemistry with the observation of dicacodyl, Me$_2$As–AsMe$_2$,[1] only two structurally authenticated examples of dicacodyl serving as a bridging ligand between two metal centres have appeared;[2] counter-intuitively, dicacodyl was the immediate precursor to neither. Cotton isolated dimeric [Cr$_2$(μ-As$_2$Me$_4$)$_2$(CO)$_8$] in unspecified yield from thermolysis of [Cr(CO)$_6$] with cacodylic acid, Me$_2$AsO$_2$H,[2a] while Vahrenkamp unexpectedly obtained [Mn$_2$(μ-AsMe$_2$)(μ-As$_2$Me$_4$)Cl(CO)$_7$] from the reaction of K[Mn(CO)$_5$] with ClAsMe$_2$.[2b] In the interim, more systematic approaches involving the coordination of pre-formed diarsines[3] or functionalisation of a pre-coordinated *diarsene*[4] have provided what remains a rather small library of diarsine-bridged bimetallics (**A**-**G**) shown in Chart 1.

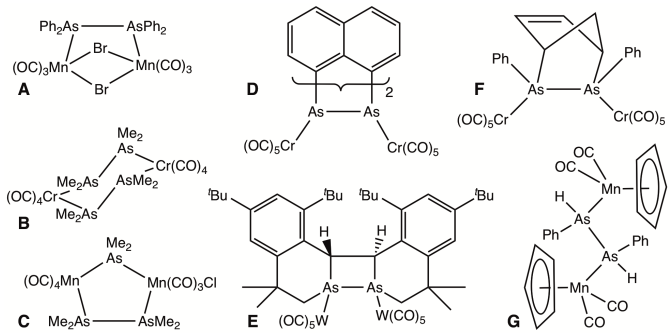

Chart 1 Structurally authenticated diarsine bridged bimetallics.[2-4]

While recently exploring the coordination of the arsolyl *metallo*-ligand [Mo(σ-AsC$_4$Me$_4$)(CO)$_3$(η^5-C$_5$H$_5$)] (**1**) to a range of unsaturated metal complexes, we observed a trace side-product **2** from the reaction of **1** with the *solvento* complex [Mn(THF)(CO)$_2$(η^5-C$_5$H$_4$Me)], alongside the major intended complex [MoMn(μ-AsC$_4$Me$_4$)(CO)$_5$(η^5-C$_5$H$_5$)(η^5-C$_5$H$_4$Me)] (**3**). The miniscule amounts obtained precluded adequate characterisation, however infrared and ^{1}H NMR data indicated a highly symmetrical species while ESI-mass spectrometry suggested the composition "(Me$_4$C$_4$As)Mn(CO)$_2$(C$_5$H$_4$Me)". Given the diamagnetism of the compound, it was tentatively formulated as the biarsolyl-bridged bimetallic species [Mn$_2${μ-(AsC$_4$Me$_4$)$_2$}(CO)$_4$(η^5-C$_5$H$_4$Me)$_2$] (**2**) by analogy with Huttner's diarsine complex [Mn$_2$(μ-As$_2$H$_2$Ph$_2$)(CO)$_4$(η^5-C$_5$H$_5$)$_2$] (**G**, Chart 1).[4] As this would constitute the first complex of a biarsolyl, and given the scarcity of bridging biarsine complexes more generally, pursuit of such a species seemed appropriate. Herein we report a strategic synthesis of **2** that provides sufficient amounts for full characterisation. Furthermore, since free biarsolyls are themselves rather rare (Chart 2) and little studied,[6] as indeed are bistibolyls and bibismolyls,[6f,7] we have explored the structure and bonding of key examples.

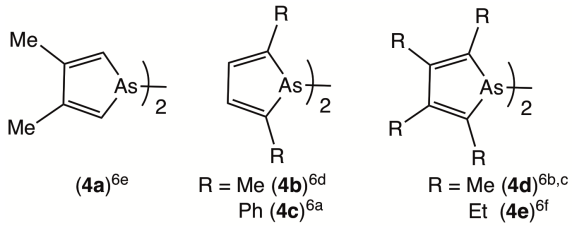

Chart 2. Previously reported biarsolyls.[6]

Results and Discussion

A Biarsolyl Complex – Suspecting that the trace side product encountered in the synthesis of the manganese complex **3**[5] was the octamethylbiarsolyl complex [Mn$_2${μ-(AsC$_4$Me$_4$)$_2$}(CO)$_4$(η^5-C$_5$H$_4$Me)$_2$] (**2**) the viability of the pruned model complex [Mn$_2${μ-(AsC$_4$H$_4$)$_2$}(CO)$_4$(η-C$_5$H$_5$)$_2$] (**5**) was computationally explored (DFT:ωB97X-D/6-31G*, Figure 1) suggesting, albeit equivocally, that it is the centrosymmetric *anti*-Mn-As-As-Mn conformer that predominates in solution (observed CH$_2$Cl$_2$: ν_{CO} = 1921vs, 1864vs cm^{-1}; hexane: ν_{CO} = 1941s, 1930vs, 1877vs cm^{-1}). No bipnictolyl bridged complexes have been previously reported however a single example of a partially reduced tetrahydrobiphospholyl bridged complex[8] [Rh$_2${μ$_2$-(PC$_4$H$_4$Me$_2$-3,4)$_2$}$_2$(η^4-cod)$_2$](BF$_4$)$_2$ (cod = cyclo-octa-1,5-diene) involves *gauche* arrangement of the dihydrophospholyl rings.

[a] Research School of Chemistry, Australian National University, Canberra, ACT. Email: a.hill@anu.edu.au.

† Electronic Supplementary Information (ESI) available: Spectroscopic, computational and crystallographic data. CCDC 2145365, 2145366, 2145368, 2145380, 2234994 and 2236821 contain the supplementary crystallographic data for this paper and are available free of charge from the Cambridge Crystallographic Data Centre.

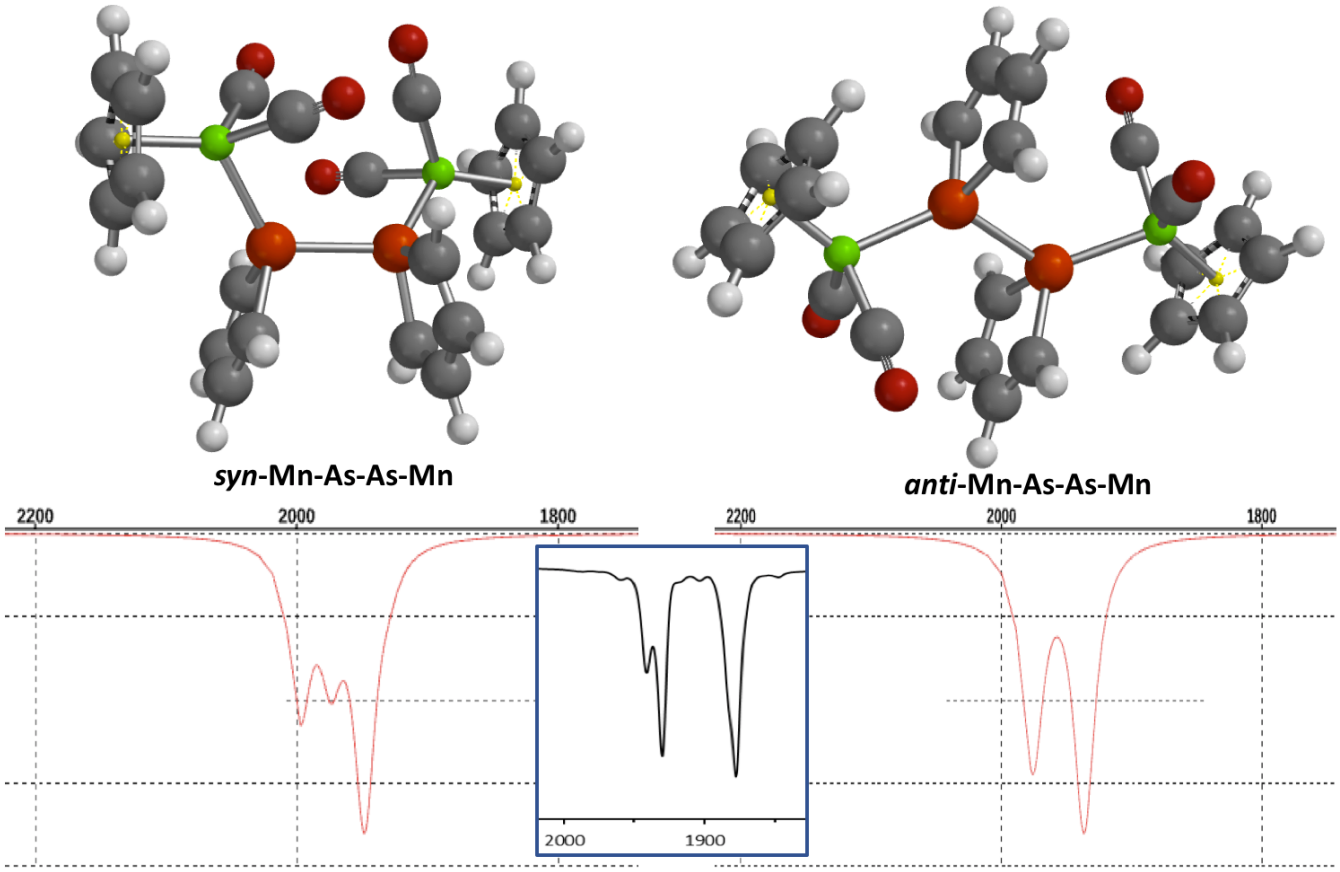

Figure 1. Optimised geometries and calculated infrared spectra (ν_{CO}, cm^{-1}) for the hypothetical biarsolyl conformeric complexes *syn*- and *anti*-$[Mn_2\{\mu\text{-}(AsC_4H_4)_2\}(CO)_4(\eta\text{-}C_5H_5)_2]$ (**5**) (ωB97X-D/6-31G*, IR scaling factor = 0.9420). Inset = experimentally determined spectrum (*n*-hexane) of side product from synthesis of **2**.

A deliberate synthesis of the presumed dimanganese complex was undertaken to confirm its formulation as $[Mn_2\{(AsC_4Me_4)_2\}(CO)_4(\eta^5\text{-}C_5H_4Me)_2]$ (**2**), to thereby provide the first example of a transition metal biarsolyl complex. The obvious approach would be addition of two equivalents of the *solvento* complex $[Mn(THF)(CO)_2(\eta^5\text{-}C_5H_4Me)]$ to the free octamethylbiarsolyl **4d** and this was indeed the route taken. The requisite biarsolyl **4d** was first described by Theopold[6b] and subsequently by Mathey[6c] *via* the routes indicated in Scheme 1.

We have made minor practical modifications to the protocols and whilst these do not involve fundamental differences to the approach or underlying chemistry, they minimise the manipulations of thermally and aerobically sensitive intermediates. Specifically, chlorotetramethylarsole was prepared directly from di-*n*-butylzirconocene without isolation of the zirconacyclopentadiene ('zirconole'). This was then divided into equal portions, the first of which was reduced (Na/Hg) to the sodium arsolide before recombining with the second portion in a Würtz-type coupling process. Amalgamated sodium proved superior to lithium wire or potassium mirrors which each led to over-reduction accompanied by grey unidentified precipitates. The product **4d** is air-sensitive as a

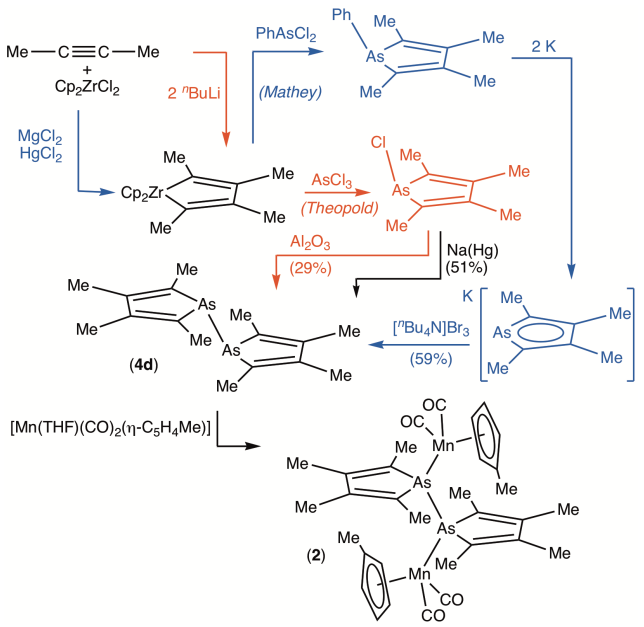

Scheme 1. Synthesis of octamethylbiarsolyl (**7Me$_8$**) based on modifications to approaches by Theopold[6b] in red and Mathey[6c] in blue. Cumulative yields given based on $[ZrCl_2(\eta^5\text{-}C_5H_5)_2]$.

solid and in solution, however, strictly anaerobic chromatography on neutral alumina with *n*-hexane eluent provided the expected biarsolyl $(AsC_4Me_4)_2$ in good yield (51% from $[ZrCl_2(\eta^5\text{-}C_5H_5)_2]$) as a yellow crystalline solid. The spectroscopic data were in agreement with those reported by Theopold,[6b] to which may now be added structural and computational data discussed below.

The addition of excess $[Mn(THF)(CO)_2(\eta^5\text{-}C_5H_4Me)]$[9] to a THF solution of **4d** provided a bright orange mixture from which a single, moderately air-stable orange product was isolated following column chromatography; IR and ^1H NMR spectra are in perfect agreement with those of the side-product mentioned above and the proposed dimeric composition was confirmed by high-resolution mass spectrometry. Despite its novelty, the $^{13}C\{^1H\}$ NMR spectrum (C_6D_6) is rather unremarkable: the four equivalent (C_{2h}) carbonyl nuclei are found at 232.4 ppm and the biarsolyl ring-carbons at 143.5 (2,5-positions) and 139.7 (3,4) ppm. The remaining carbon environments are so similar to those of **2** that no comment is warranted. While the infrared data discussed above point to an *anti*-Mn–As–As–Mn arrangement, these and the NMR data are not definitive. Single crystals were however obtained by slow evaporation of a benzene solution and the emergent structural model is shown in Figure 2.

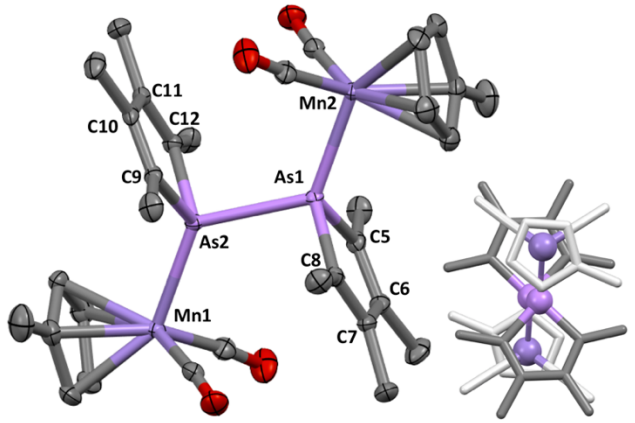

Figure 2. Molecular structure of $[Mn_2\{(AsC_4Me_4)_2\}(CO)_4(\eta^5\text{-}C_5H_4Me)_2]$ (**2**) in a crystal (50% displacement ellipsoids, hydrogen atoms omitted). Inset = view along As···As vector to demonstrate *antiperiplanar* arrangement of manganese centres.

The molecular structure determination confirmed the expected dimanganese biarsolyl complex formulation. It should be noted that although the solid-state structure ostensibly *appears* to contain an inversion centre (at the midpoint of the diarsine bond), no such symmetry element is crystallographically imposed upon the structural model and a satisfactory solution was obtained in a non-centrosymmetric space group (monoclinic *Cc*; R_1 = 0.024). Attempts to account for missing symmetry by model refinement in centric monoclinic space groups (*e.g.*, $P2_1/c$, $C2/c$) did not arrive at plausible structure solutions. The superficial centrosymmetric nature of the *anti*-conformation appears to be coincidental since the two *pseudo* halves of the molecule do indeed exhibit subtle differences from one another *viz*. Mn1-As1 2.3234(5) Å and Mn2-As2 2.3147(5) Å. The diarsine bond measures 2.4610(5) Å (*cf.* $[Mn_2(\mu\text{-}PhHAsAsPhH)(CO)_4(\eta^5\text{-}C_5H_5)_2]$[4] As–As = 2.462(1) Å) which is slightly elongated compared to the free ligand *gauche*-**4d** (2.4462(4) Å;). The mean As→Mn dative bond of 2.3190(7) Å is also in accord with that of ($[Mn_2(\mu\text{-}PhHAsAsPhH)(CO)_4(\eta^5\text{-}C_5H_5)_2]$[4] Mn-As = 2.319(2) Å). The As-As-Mn angle of *ca* 123° is typical of other mono-arsolyl bridged complexes devoid of metal-metal bonding[5] and the arsenic(II) atom(s) are essentially contained within the mean plane of the butadiene, being displaced by only 0.6°. Distances and angles about the arsole ring are crystallographically indistinguishable from other σ-bound AsC_4Me_4 ligands.[5,10]

The *antiperiplanar* disposition of manganese centres with respect to the As–As bond of **2** raises the question of whether the biarsolyl bridge might support a degree of intermetallic communication. This would appear to be the case when one considers the hypothetical model complex *anti*-$[Mn_2\{(AsC_4H_4)_2\}(CO)_4(\eta^5\text{-}C_5H_5)_2]$ (*anti*-**5**), selected molecular orbitals of which (Figure 3, HOMO-8,12, 13, 14 and 16) indicate electronic communication along the Mn–As–As–Mn spine. Details of the full permethylated molecule *anti*-$[Mn_2\{(AsC_4Me_4)_2\}(CO)_4(\eta^5\text{-}C_5H_5)_2]$ are presented in the ESI, however as inclusion of methyl groups has a negligible effect on the core geometry or resulting charges and bond orders, the visually simpler *anti*-**5** is described here.

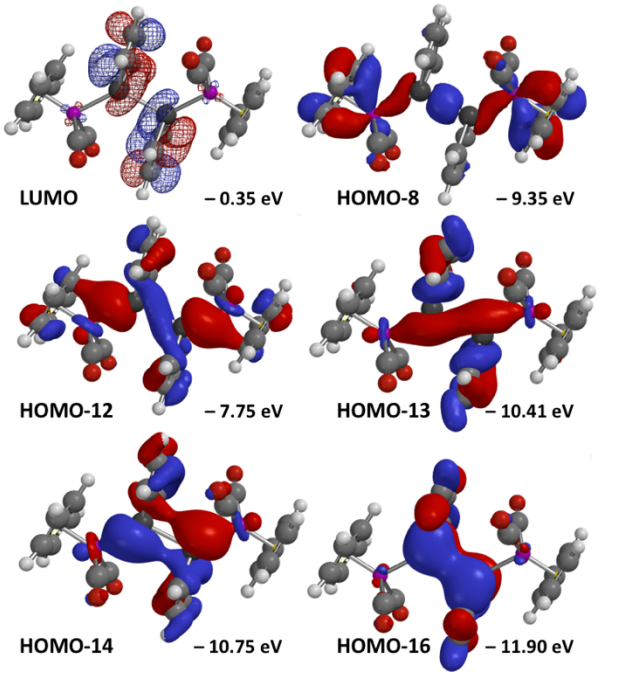

Figure 3. Selected molecular orbitals for hypothetical $[Mn_2\{(AsC_4H_4)_2\}(CO)_4(\eta^5\text{-}C_5H_5)_2]$ that suggest communication pathways between the manganese centres (DFT: ωB97X-D/6-31G*/gas-phase).

Figure 3 also depicts the LUMO which is exclusively associated with the biarsolyl bridge and has As–As σ*-antibonding character, *i.e.*, two electron reduction would be

expected to result in cleavage to form the mononuclear anion $[Mn(AsC_4H_4)(CO)_2(\eta^5\text{-}C_5H_5)]^-$ although this possibility has yet to be explored with real **2**.

Free Biarsolyls.

To provide context for the biarsolyl complex **2**, it is useful to consider structural and computational data for free biarsolyls. The parent biarsolyl $(AsC_4H_4)_2$ (**4f**) has not been reported and given the proclivity of arsoles to enter into cycloaddition reactions, it is likely to have limited longevity *ex silico*. Nevertheless, **4f** serves to illustrate the frontier orbitals of interest (vide infra) for more heavily substituted derivatives **4a-e** for which no theoretical investigations have appeared.[11] Prior to this work only a single biarsolyl had been structurally characterised. Ashe prepared the 2,2'5,5'-tetramethylbisarsolyl $(AsC_4H_2Me_2\text{-}2,5)_2$*(As-As)*[6d] with a view to investigating the origins of the unusual thermochromic behaviour of the antimony analogue. It transpired that unlike the purple-blue bistibolyl, the yellow biarsolyl displayed no notable thermochromic behaviour, an observation that was attributed to the difference in the solid state structures. The centrosymmetric bistibolyl antimony atoms align in a linear chain with short intermolecular Sb···Sb contacts[11a] (what might now be referred to as pnictogen bonding[11c]) while the discreet biarsolyl adopts a *gauche* C_2-symmetric geometry with no intermolecular interactions of note.

Structural Studies of Biarsolyls – as part of a broader study of the chemistry of arsoles detailed elsewhere, we have encountered further examples of biarsolyls that we have been able to structurally characterise: the 2,2'5,5' tetraphenyl derivative $(AsC_4H_2Ph_2\text{-}2,5)_2$ (**4c**)[6a] and the octamethyl $(AsC_4Me_4)_2$ (**4d**) each of which has been described previously by Märkl[6a] and Theopold,[6b] respectively. To this collection we may add the octaphenyl derivative $(AsC_4Ph_4)_2$ (**4g**) which arose inadvertently from the reaction of $[Cr(Sn^nBu_3)_3(\eta^5\text{-}C_5H_5)]$ and $ClAsC_4Ph_4$.[10] The molecular structures of these biarsolyls are summarised in Figures 4-6 while salient data are collated in Table 1 alongside those for $(AsC_4H_2Me_2\text{-}2,5)_2$ (**4b**).[6d] Table 1 also includes geometrical parameters that we have derived computationally (*vide infra*) which at the ωB97X-D/6-31G* level of density functional theory appear to adequately reproduce the core geometries, obviating any distortions that might arise from crystal packing effects.

From these data it emerges that two geometries are possible in which the centroids of the arsolyl rings lie at dihedral angles that are either *gauche* (**4b**, **4d**, **4g**) or *antiperiplanar* (**4c**) with respect to the As–As bond. In the case of **4c**, the centroids are strictly *antiperiplanar* by virtue of the crystallographic ($P2_1/c$) inversion centre that bisects the As–As bond, such that the arsolyl planes are necessarily parallel. This conformation is also found for crystallographically centrosymmetric (*P*-1) tetramethyl-bistibolyl,[7a] and bibismolyl,[7e] noting that the covalent radii sums for Sb–Sb (2.78) and Bi–Bi (2.96 Å) bonds exceed that

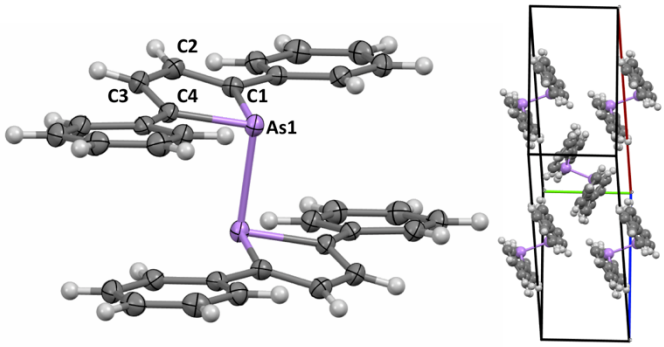

Figure 4. Molecular structure of **4c** in a crystal (50% displacement ellipsoids, only half the molecule is crystallographically unique due to an inversion centre bisecting the As1–As1 bond). For selected bond lengths and angles see Table 1.

for As–As (2.38 Å) which should help to ameliorate steric interactions. This orientation does allow the antimony and bismuth centres to enter into secondary bonding,[12] however no such interaction is evident in the case of **4c**, with the closest and clearly non-bonding intermolecular As···As separation being 4.9482(2) Å (Figure 4 inset). The *intra*molecular As–As bond (2.461(3)Å) in **4c** is somewhat longer than in **4a** (2.438(1)Å),[6d] but comparable to simple diarsines devoid of steric encumbrance $R_2As\text{–}AsR_2$ (R = Ph 2.4603(4),[13] CF_3 2.463(1),[14] CH_3 2.429(1) Å[15]), though this may be elongated in response to steric clutter (R = $C_6H_2Me_3$-2,4,6 2.472(3),[16] $CH(SiMe_3)_2$ 2.538-2.592[17]). Exocyclic angles at arsenic for structurally characterised arsoles are typically close to 100° due to reduced *s*-character in the arsenic bonding,[11,18] and for **4g** these angles are even closer to orthogonality (As1–As1-C1 = 95.81(5), As1-As1-C4 = 94.26(5)°).

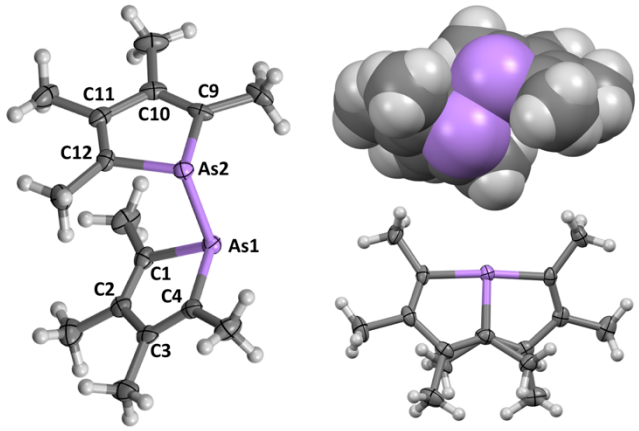

Figure 5. Molecular structure of **4d** in a crystal (50% displacement ellipsoids). Insets = space-filling representation and view along the As···As vector. For selected bond lengths and angles see Table 1.

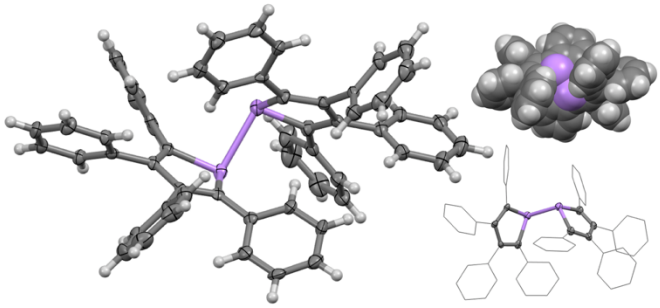

Figure 6. Molecular structure of **4g** in a crystal (50% displacement ellipsoids). Insets = space-filling representation and wire-frame view emphasising inner core geometry. For selected bond lengths and angles see Table 1.

Table 1. Selected geometric parameters for free biarsolyls.

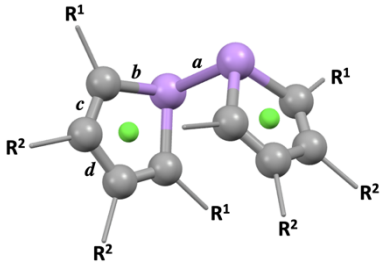

R¹	R²	*a* [Å]	*b* [Å]	*c* [Å]	*d* [Å]	Σ°As[a] [°]	Dihed[b] [°]	∠planes[c] [°]
Experimental (X-ray crystallography)								
Me[6a]	H **4b**	2.438	1.940	1.336	1.444	286.6	71.1	32.9
Ph	H **4c**	2.464	1.957	1.353	1.443	276.7	180.0[d]	0.0[d]
Me	Me **4d**	2.446	1.929	1.341	1.481	285.4	88.2	29.7
Ph	Ph **4g**	2.474	1.943	1.361	1.478	295.7	104.2	48.4
Calculated (DFT:ωB97X-D/6-31G*)								
H	H **4f**	2.460	1.938	1.348	1.461	274.4	173.1	0.9
Me	H **4b**	2.459	1.953	1.348	1.457	280.4	179.2	1.4
Me	Me **4d**	2.462	1.935	1.352	1.480	282.6	67.4	26.2
Me	Me **4d**	2.463	1.938	1.352	1.480	280.2	161.6	9.9
Ph	Ph **4g**	2.431	1.955	1.349	1.470	304.4	112.9	46.1
ᵗBu	Me **4h**	2.495	1.939	1.357	1.488	291.3	94.9	33.5

[a]Angle sum at arsenic. [b]Torsional angles between arsolyl ring centroids and As–As axis. [c]Angle between arsolyl planes. [d]Crystallographically imposed in $P2_1/c$.

The planes of the *ortho*-phenyl rings of **4c** are canted (19.7°) from the arsolyl plane so as to allow π-stacking interactions with the ring on the adjacent arsolyl (inter-centroid distance 3.64 Å), though since this separation exceeds twice the van der Waals radius for carbon (3.4 Å), the individual interactions must be considered modest. Indeed, this favourable interaction appears insufficient to overcome the steric encumbrance in the perphenylated example **4g**, which adopts a *gauche* conformation with neither C–H···π nor π···π stacking interactions being evident between adjacent molecules. As is generally the case for the small number of structurally characterised arsoles, the angles at arsenic are contracted from the tetrahedral ideal, while the C–As–C angles fall well below the pentagonal ideal (108°) reflecting the longer C–As bonds. For the *gauche* examples the mean angle that the As–As bond makes with the C2-C5 centroids is quite obtuse (**4d** 102.1/109.3°, **4a** 107.3/106.1, **4g** 114.2/114.0°), while for *anti*-**4c** it is slightly contracted (98.2°), again most likely to foster the π-stacking interaction of the phenyl substituents. Bonding within the arsolyl ring reflects considerable butadiene rather than aromatic character with C–C separations approaching values typical of localised double (***c***: 1.34-1.36 Å) and single (***d***: 1.44-1.48 Å) sp^2-sp^2 bonds. The As–As bond lengths are sensitive to inclusion of sterically demanding *ortho*-phenyl substituents leading to lengthening. In the case of **4g**, this also results in a splaying of the two arsole ring planes (46.1°).

For both **4d** and **4g** the orientation of the two AsC_4 rings in the solid state is *gauche* so that the molecule has approximate C_2-symmetry with the alternative enantiomer being in each case generated by crystallographic symmetry. In addition to favouring the *gauche* conformation, introduction of steric bulk with substitution at all of the eight ring positions results in (i) a lengthening of the As–As bond and (ii) splaying of the individual arsolyl rings away from the parallel arrangement in *anti*-**4c**.

Computational analysis of biarsolyls. Geometric optimisation (DFT: ωB97X-D/6-31G*) of $(AsC_4H_4Me_2)_2$ (**4b**) affords both the *gauche* C_2-**4b** and centrosymmetric (*anti*) C_{2h}-**4b** conformers. In the gas phase, the former lies some 17.9 kJmol^{-1} lower in energy than the latter, *i.e.*, at room temperature the *gauche* form will predominate (K(C_2-**4b** → C_{2h}-**4b**) = 7.4 x 10^{-4}) with Ashe noting, however, that rotation about the As–As bond is not arrested on the ^{1}H NMR timescale at –100 °C (360 MHz).[6d] At this level of theory, the C_2 and C_{2h} conformers are calculated to have $\nu_{As\text{-}As}$ absorptions at 240 and 239 cm^{-1}, respectively, in both the infrared (weak) and (more intense) Raman spectra. These correspond to Ashe's experimental observation of a Raman band at 241 cm^{-1} in the solid state and little changed at 239 cm^{-1} as a liquid. At this level of theory the essentially pure A_g(As–As) mode of C_{2h}-H_2As–AsH_2 has ν_{AsAs} = 253 cm^{-1} as an intense Raman band that is IR-inactive (Löwden bond order: 1.17). Thus vibrational spectroscopy would *not* be expected to definitively differentiate between the two conformers. Analysis of the parent hypothetical biarsolyl $(AsC_4H_4)_2$ (**4f**) devoid of any appreciable steric influences from the substituents suggests that the *anti*-C_{2h} (ν_{AsAs} = 227 cm^{-1}) and *gauche*-C_2 (ν_{AsAs} = 223 cm^{-1}) conformers of **4f** are of equal energy ($\Delta G \approx 0.1$ kJmol^{-1}), *i.e.*, the geometric preference for C_2-**4b** over C_{2h}-**4b** would appear to be entirely steric in origin and presumably exacerbated for **4d** and **4g**.

The frontier orbitals of *anti*-C_{2h} and *gauche*-C_2 conformers of **4f** are shown in Figure 7, from which it is apparent that for both geometries the HOMO and HOMO-1 are almost equal in energy though these reverse in order for the two conformers. The HOMO of the *gauche* rotamer and the HOMO-1 of the *anti* conformer correspond to the arsenic-independent butadiene-like orbital that might be employed in Diels-Alder type cyclo-addition reactions – *except that none have been reported to date for biarsolyls*.

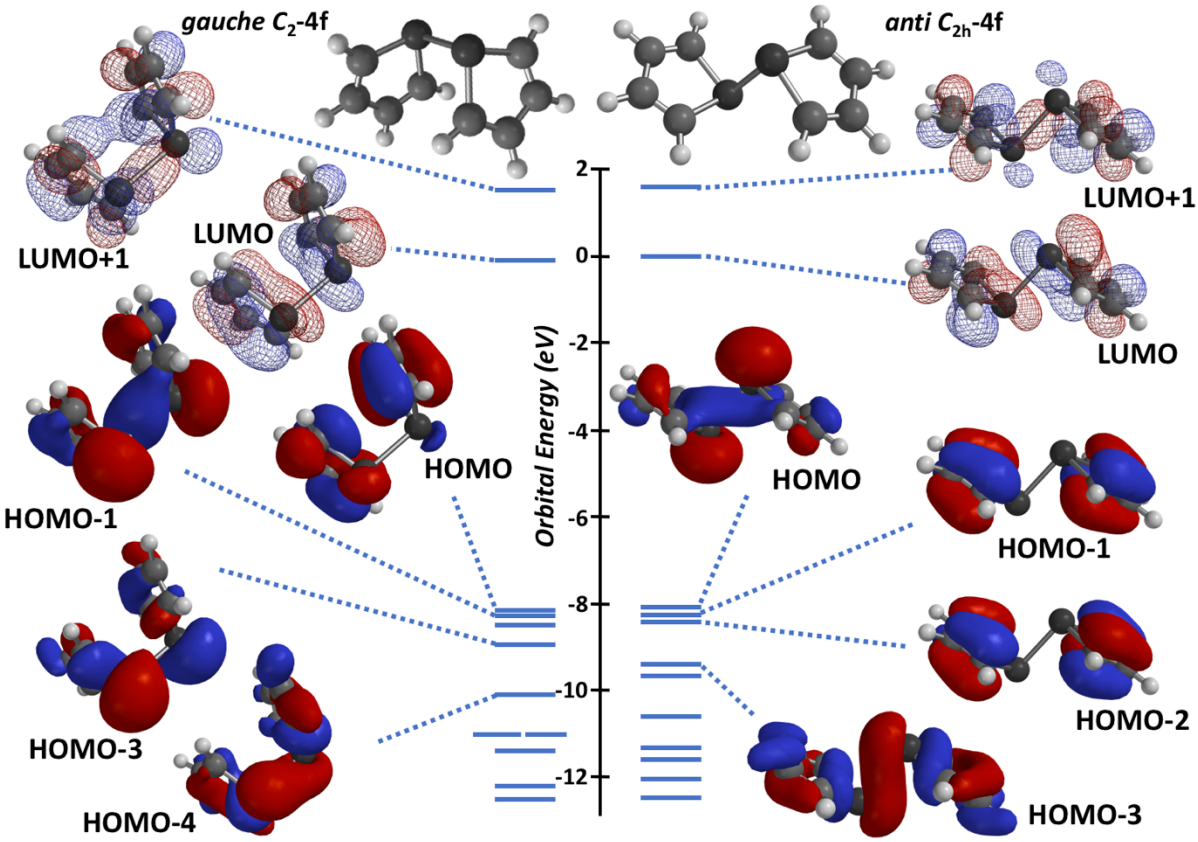

Figure 7. Molecular orbitals of interest for *gauche* C_2-**4f** (left) and *anti* C_{2h}-**4f** (right) conformers of biarsolyl $(AsC_4H_4)_2$*(As–As)* (ωB97X-D/6-31G*/gas phase).

For centrosymmetric C_{2h}-**4f**, the HOMO and HOMO-3 both contribute to As–As σ-bonding and the LUMO corresponds to the As–As σ-antibonding orbital. For *gauche* C_2-**4f** the σ-bonding orbitals are HOMO-1 and HOMO-4 while the LUMO remains As–As σ-antibonding.

For C_2-**4b**, the yellow colour originates from the visible tail of the HOMO-LUMO (calc. 96%, 322 nm) transition and since the HOMO is 'butadiene-like' while the LUMO has a substantial As–As σ* antibonding character (Figure 7), it may be assumed the biarsolyls will be prone to photochemical cleavage of the As–As bond. Furthermore, 2-electron reduction is likely to cleave the As–As σ-bond, corresponding to the microscopic reverse of its synthesis from oxidation of the 2,5-dimethylarsolide anion.[6a] Consistent with this, beginning with the atomic coordinates of neutral **4d**, geometrical optimisation of the analogous dianion [**4d**]$^{2-}$ results, unsurprisingly, in the two arsolyl groups taking flight in opposite directions along the As···As vector, thereby notionally mimicking reductive cleavage. The atom-condensed Fukui functions[19] are presented in Figure 8 alongside the natural atomic charges and Löwdin bond orders for both the permethylated **4d** and the hypothetical parent biarsolyl **4f**. For the simple parent *anti*-**4f** in frontier-orbital controlled reactions, while the arsenic centres are clearly the sites most susceptible towards electrophilic attack (f^- = 0.296, see also HOMO Figure 7) it would appear that with nucleophiles the 2,5-carbon atoms are also likely to be prone to attack ($f^+(C^{2,5})$ = 0.260 *cf.* f^+(As) = 0.143). The charges on adjacent carbon centres (–0.58) perhaps suggest that charge-control may well play a role in directing nucleophilic attack (Figure 9. Some ambident behaviour is therefore perhaps to be expected.

In passing, and with computational data for biarsolyls in hand, it seemed appropriate to briefly consider together the remaining pnictogens. For the heavier pnictogens, only $(AC_4H_2Me_2\text{-}2,5)_2$, $(AC_4Me_4)_2$, $\{AC_4(SiMe_3)_2\text{-}2,5\text{-}Me_2\text{-}3,4\}_2$ (A = Sb, Bi) and $(BiC_4Me_2\text{-}2,5\text{-}C_2H_4\text{-}3,4)_2$ have been reported[7] with only $(AC_4H_2Me_2\text{-}2,5)_2$ (A = Sb,[7a] Bi[7e]) having been structurally characterised. Lohr briefly considered the parent bibismolyl $(BiC_4H_4)_2$ employing semi-empirical methods[19] while in the context of exploring bistibolyl thermo-chromicity, Hoffmann considered $(SbC_4H_4)_2$ at the extended Hückel level of theory.[8] For consistency, we survey here the compounds $(AC_4H_4)_2$ (A = N, P, As, Sb, Bi) at the ωB97X/6-31G*/LANL2DZ(Sb,Bi) level of density functional theory (Figure 10). The real-world molecules $(AC_4Me_4)_2$ (A = N, P, As, Sb) are relegated to the supporting information because permethylation somewhat compromises visual clarity and because $(BiC_4Me_4)_2$ is omitted due to bismuth not being implemented in the ωB97X-D functional within *SPARTAN20*.[23] Permethylation, whilst raising the energies of all orbitals, has remarkably little effect on the topologies of the frontier orbitals. Thus the hypothetical parent molecules, when coordinated to a metal, would be expected to be somewhat poorer σ-donors

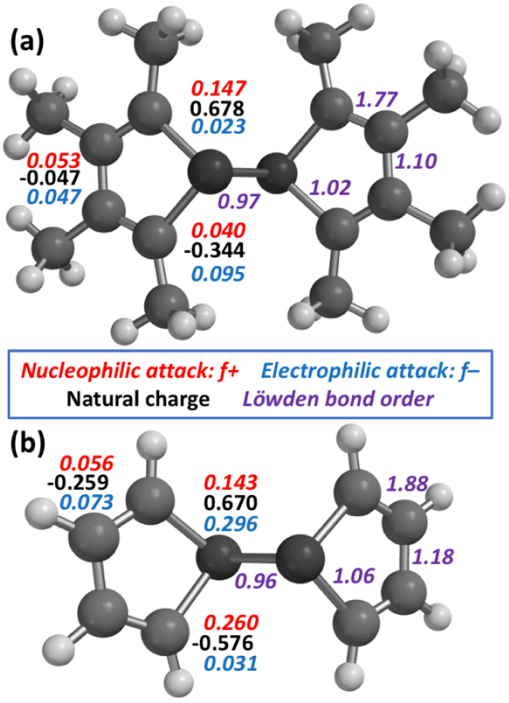

Figure 8. Natural charges (black), Löwden bond orders (purple) and atom-condensed Fukui functions for nucleophilic (red, f^+) and electrophilic attack (blue, f^-) for (a) octamethylbiarsolyl (**4d**) and (b) the parent biarsolyl (**4f**).

and better π-acceptors than their octamethyl analogues. As a test example, comparison of results for $(AsC_4Me_4)_2$ (see ESI) obtained for functionals with (ωB97X-D) and without (ωB97X) dispersion correction indicates that this omission does not significantly perturb the geometry, charges or bond-orders that result.

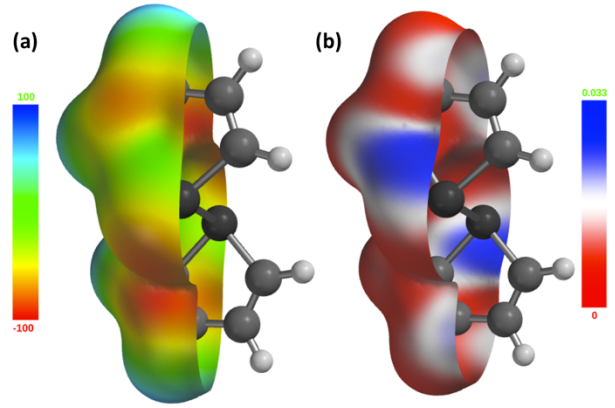

Figure 9. (a) Electrostatic potential (–100 to +100 kJ) and (b) LUMO (0 to 0.033 √e/au²) maps (0.002 e/au³ surfaces) for parent biarsolyl **4f**.

Unsurprisingly, the proclivity for first row elements to take part in effective pπ-pπ overlap ensures that the drive towards aromaticity in the bipyrrolyl (A = N) ensures that the nitrogen atoms are trigonal with a D_{2d} geometry. The permethylated bipyrollyl $(NC_4Me_4)_2$ (see ESI) involves the additional steric conflict presented by the 2,5-methyl substituents such that the computationally derived D_{2d} geometry is much the same as has been experimentally established.[23] As such, with the current focus on the donor properties of the pnictogen, bipyrollyls fall outside the present discussion.

In all cases, geometry minimisation delivers the *gauche* conformer as the lowest energy, as is also the case for the permethylated examples (ESI). The pnictogen-pnictogen Löwdin bond order is essentially invariant down the series, remaining close to unity (0.97-1.03), while the natural atomic charge on the pnictogen monotonically increases but only slightly from +0.61(P) to +0.81 (Bi). For the simple known molecules AMe_3 (A = P, As, Sb, Bi) at this same level of theory, the natural atomic charge on descending the group increases more significantly from +0.86 (P) to +1.23 (Sb, Bi) while the energy of the primarily lone pair on the pnictogen is essentially invariant (*ca* –8.5 eV). For *gauche*-$Me_2A–AMe_2$ the charge on the pnictogen increases from +0.55 (P) to +0.79 (Bi). The energy of the π-acceptor degenerate LUMO pair decreases quite markedly from +4.1 (PMe_3) to +2.5 eV suggesting an increase in π-acidity when acting as a ligand, notwithstanding decreased dπ-pπ overlap due to the progressive lengthening of the metal–A bond. In contrast not only are the energies of the LUMO and LUMO+1 for the bipnictolyls little changed on descending the group, their spatial disposition is not well-suited for them to serve as π-acceptors. Three molecular orbitals have significant contributions from the pnictogen 'lone pair' and to varying extents these all increase in energy upon descending the group. The HOMO-1 for the diphospholyl corresponds to the HOMO for the remaining bipnictolyls (in red, Figure 10) and this increases moderately in energy down the group, having both lone-pair and pnictogen-pnictogen σ-bonding character. The HOMO-3 series (pnictogen lone pairs) is essentially invariant down the group while the HOMO-4 represents a combination of both pnictogen-carbon σ-bonding and slightly helical pnictogen-pnictogen overlap. Notably, this orbital has the most pronounced destabilisation down the group. Taken together these results would suggest that on descending group 15, the pnictogen becomes more nucleophilic and a better σ-donor, which seems counter-intuitive given that for simple phosphines *vs* bismuthines the σ-basicity is considered to decrease. We attribute this to the loss of some degree of charge stabilisation due to the unsaturated heterocycle ring, which become progressively less effective down the group due to poorer pπ-pπ overlap.

Conclusions

Whilst μ-arsolyl bridged bimetallic assemblies have only recently begun to attract attention,[5,20] the possibility of biarsolyls also being able to serve as bridging ligands is reported here for the first time. Though prompted by serendipitous appearance, once recognised as such it was a simple task to develop an intentional synthetic route to such a complex, that also promises a degree of generality. The intriguing possibility that biarsolyl bridges might allow some degree of intermetallic communication has been mooted

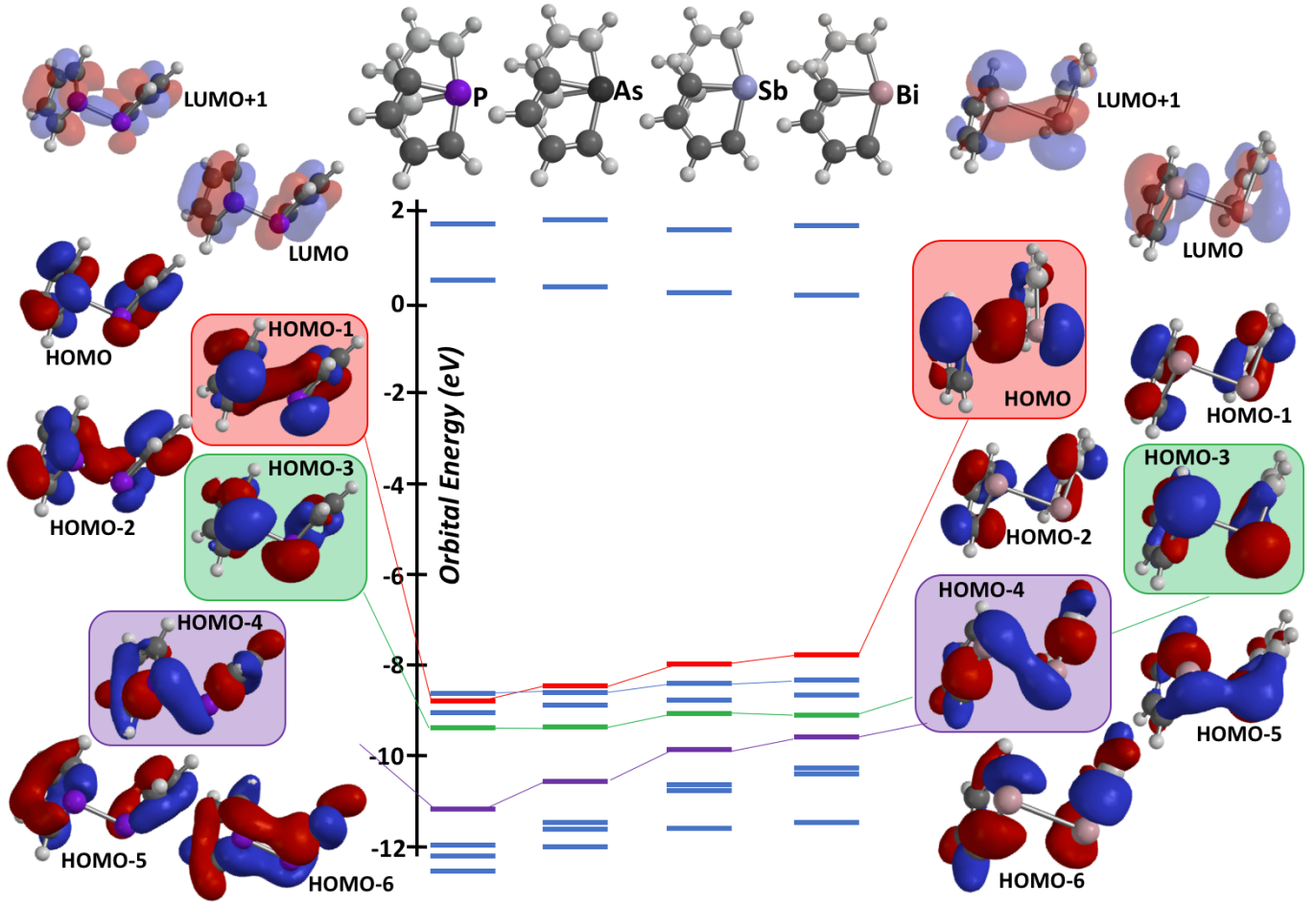

Figure 10. Frontier orbitals of interest for the hypothetical molecules *gauche*-$(AC_4H_4)_2$*(A-A)* (A = P, As, Sb, Bi; ωB97X/6-31G*/LANL2Dζ(Sb, Bi)/gas phase. Similar results are presented in the Electronic Supporting Information for $(AC_4Me_4)_2$*(A-A)* (A = P, As, Sb; ωB97X-D/6-31G*//LANL2Dζ(Sb). The orbital topologies are shown for the two extreme members $(PC_4H_4)_2$ (left) and$(BiC_4H_4)_2$ (left).

here but now awaits experimental verification. Extension to the heavier pnictogens, *i.e.*, bridging bistibolyls and bibismolyls would seem plausible, while noting that simple bridging stibolyl or bismolyl ligands have yet to be reported.

Author Contributions

RMK was responsible for the design and execution of the experimental research, the acquisition and critical analysis of the characterisation data and compilation of the original draft. AFH was responsible for funding acquisition, project conceptualisation and administration, validation and refinements to the manuscript.

Acknowledgements

We gratefully acknowledge the Australian Research Council (DP200101222 and DP230199215) for funding.

Conflicts of interest

There are no conflicts to declare.

Experimental

Experimental protocols, instrumentation, crystallographic and computational methods are provided in the accompanying Electronic Supporting Information.

Notes and references

1 (a) Essay: D. Seyferth, 2001, **20**, 1488-1498. (b) L. C. Cadet de Gassicourt, *History of a fuming liquor drawn from arsenic,* Memoires of Mathematics and Physics presented to the Royal Academy of Sciences, 1760, **3**, 623.

2 (a) F. A. Cotton and T. R. Webb, *Inorg. Chim. Acta*,1974, 10, 127-131. (b) E. Rottinger, A. Trenkle, R. Muller and H. Vahrenkamp, *Chem. Ber.*, 1980, **113**, 1280-1289.

3 (a) F. Calderazzo, R. Poli, D. Vitali, J. D.Korp, I. Bernal, G. Pelizzi, J. L. Atwood and W. N. Hunter, *Gazz. Chim. Ital.*,

1983, **113**, 761-771. (b) K. Dzialkowski, A. Gehlhaar, C. Wolper, A. A. Auer and S. Schulz, *Organometallics*, 2019, **38**, 2927-2942. (c) M. D. Francis, D. E. Hibbs, M. B. Hursthouse, C. Jones and K. M. A. Malik, *Chem. Commun.*, 1996, 631-632.
4 (a) I. Jibril, L.-R. Frank, L. Zsolnai, K. Evertz and G. Huttner, J. Organomet. Chem., 1990, **393**, 213-225. (b) G. Huttner, H.-G. Schmid and H. Lorenz, *Chem. Ber.*, 1976, **109**, 3741-3749.
5 R. M. Kirk and A. R. Hill, *Dalton Trans.*, 2023, **52**, 10190-10196.
6 (a) G. Märkl and H. Hauptmann, *Angew. Chem., Int. Ed. Engl.*, 1972, **11**, 439-440. (b) S. C. Sendlinger, B. S. Haggerty, A. L. Rheingold and K. H. Theopold, *Chem. Ber.*, 1991, **124**, 2453-2456. (c) F. Nief, L. Ricard and F. Mathey, *Polyhedron*, 1993, *12*, 19-26. (d) A. J. Ashe, W. M. Butler and T. R. Diephouse, *Organometallics*, 1983, **2**, 1005-1008. (e) F. Nief and L. Ricard, *Organometallics*, 2001, **20**, 3884-3890. (f) M. Westerhausen, C. Giuckel, H. Piotrowski, P. Mayer, M. Warchhold and H. Nöth, *Z. Anorg. Allg. Chem.*, 2001, **627**, 1741-1750.
7 (a) A. J. Ashe, W. Butler and T. R. Diephouse, *J. Am. Chem. Soc.*, 1981, **103**, 207-209. (b) R. E. v. H. Spence, D. P. Hsu and S. L. Buchwald, *Organometallics*, 1992, **11**, 3492-3493. (c) A. J. Ashe and T. R. Diephouse, *J. Organomet. Chem.*, 1980, **202**, C95-C98 (d) A. J. Ashe and E. G. Ludwig, *J. Organomet. Chem.*, 1986, **303**, 197-204. (e) A. J. Ashe, J. W. Kampf, D. B. Puranik and S. M. Al-Taweel, *Organometallics*, 1992, **11**, 2743-2745. (f) R. E. v. H. Spence, S. L. Buchwald and J. F. Richardson, *Acta Chem. Scand.*, 1993, **47**, 326-329.
8 A. L. Crumbliss, R. J. Topping, J. Szewczyk, A. T. McPhail and L. D. Quin, *J. Chem. Soc., Dalton Trans.*, 1986, 1895-1899.
9 B. J. Frogley, A. F. Hill, H. Onagi and L. J. Watson, *Dalton Trans.*, 2022, **51**, 17354-17360.
10 R. M. Kirk and A. F. Hill, manuscript in preparation.
11 The heavier distibolyl 2,2'5,5'-tetramethyldistibolyl has been considered in the context of unusual thermochromic behaviour in the solid state: (a) T. Hughbanks, R. Hoffmann, M.-H. Whangbo, K. R. Stewart, O. Eisenstein and E. Canadell *J. Am. Chem. Soc.*, 1982, **104**, 3876-3879. (c) Commentary on pnictogen bonding: A. Varadwaj, P. R. Varadwaj, H. M. Marques and K. Yamashita, *Inorganics* 2022, **10**, 149.
12 S. Schenier, *Acc. Chem. Res.*, 2013, **46**, 280-288.
13 W. S. Tay, X.-Y. Yang, Y. Li, S. A. Pullarkat, P.-H. Leung, *Dalton Trans.*, 2019, **48**, 4602-4610.
14 G. Becker, W. Golla, J. Grobe, K. W. Klinkhammer, D. Le Van, A. H. Maulitz, O. Mundt, H. Oberhammer and M. Sachs, *Inorg. Chem.*, 1999, **38**, 1099-1107.
15 O. Mundt, H. Riffel, G. Becker, A. Simon, *Z. Naturforsch.*, 1988, **43B**, 952-958.
16 H. Chen, M. M. Olmstead, D. C. Pestana and P. P. Power, *Inorg. Chem.,* 1991, **30**, 1783-1787.
17 H. Chen, M. M. Olmstead, D. C. Pestana and P. P. Power, *Inorg. Chem.,* 1991, **30**, 1783-1787.
18 S. L. Hinchley, C. A. Morrison, D. W. H. Rankin, C. L. B. Macdonald, R. J. Wiacek, A. Voigt, A. H. Cowley, M. F. Lappert, G. Gundersen, J. A. C. Clyburne and P. P. Power, *J. Am. Chem. Soc.,* 2001, **123**, 9045-9053
19 (a) R. G. Parr and W. Yang, *J. Am. Chem. Soc.*, 1984, **106**, 4049-4050. (b) W. Yang and W. J. Mortier, *J. Am. Chem. Soc.*, 1986, **108**, 5708-5711.
20 R. M. Kirk and A. F. Hill, *Chem. Sci.*, 2022, **13**, 6830-6835.
21 L. L. Lohr and A. J. Ashe, *Organometallics*, 1993, **12**, 343-346.
22 *Spartan 20*® (2020) Wavefunction, Inc., 18401 Von Karman Ave., Suite 370 Irvine, CA 92612 U.S.A.
23 N. Kuhn, H. Kotowski, M. Steimann, B. Speiser, M. Wurde and G.Henkel, *J. Chem. Soc., Perkin Trans. 2*, 2000, 353-363.

Table of Contents Text

The first μ-biarsolyl complex is described and discussed in the context of structural and computational studies of free biarsolyls.

Table of Contents Graphic